

ATLAS Beamline Tuning and Characterization

RAHEEM BARNETT

*Princeton University
Argonne National Laboratory*

August 16, 2016

Abstract

A study of ATLAS focusing element strengths from the Low Energy Beam Transport line (LEBT) through the Positive Ion Injector (PII) and the PII to Booster line (P2B) was conducted to determine where measured intensity loss and instability were originating. Data collected during runs on March 10th 2016 was used to constrain and guide the TRACK simulations. Optimizations of the simulations were performed to better match the transmission data. A lower voltage solution was found for the LEBT quadrupoles that reduced the rms normalized beam emittance by 31.8% in both transverse planes. In order to measure the emittance at the end of the RFQ, quadrupole scan data was taken using a quadrupole doublet and Beam Profile Monitor (BPM) at the end of P2B with deactivated PII accelerating cavities. A data analysis script was written in MATLAB to automate the emittance calculation. The script was tested against simulation to within 1% accuracy.

I Introduction

The ATLAS Accelerator The Argonne Tandem Linear Accelerating System (ATLAS) is a user facility capable of delivering 7-17MeV/u heavy-ion beams of elements from hydrogen to uranium with a mass-to-charge ratio of up to 6. The beamline consists of sequential sections with focusing elements that must be tuned to maximize the beam transmission and ensure the beam matches the acceptance of components along the accelerator.

Overview of the beamline sections. The first section, the Low Energy Beam Transport line (LEBT), carries the beam at 0.0305MeV/u without acceleration from the ion source and injector to the Radio Frequency Quadrupole (RFQ) and consists of three quadrupole doublets and one quadrupole triplet. The next section is the RFQ which simultaneously bunches, focuses, and accelerates the beam to 0.294MeV/u. Following the RFQ is the Positive Ion Injector, a superconducting radio frequency (SRF) linac composed of three cryostat modules that in total contain fifteen accelerating cavities and eleven focusing solenoids. The section from PII to the Booster superconducting linac is the PII to Booster line (P2B),

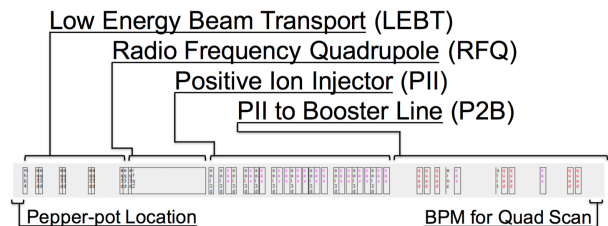


Figure 1: Relevant sections of ATLAS beamline.

containing two bunching cavities, two quadrupole doublets, and one quadrupole triplet.

ATLAS March tests. In March of 2016 runs were conducted to determine how the accelerator handles high intensity beams. Beam currents from 52nA to 5.2 μ A were tested. The data used in this analysis was from March 10th, when a quadrupole scan was conducted with PII accelerating cavities deactivated in order to measure the emittance at the exit of the RFQ. It was found that the transmission values in P2B were lower than what should have been achievable. Only 90.3% of the beam made it through P2B. Since P2B is a beam transport line and the accelerating cavities after the RFQ were all off, it

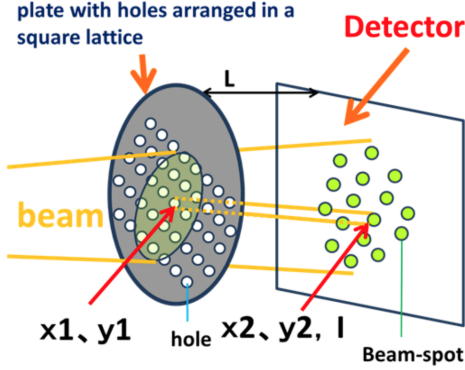


Figure 2: Schematic of a pepper-pot detector. [1]

should have been possible to achieve 100% transmission through P2B. The analysis in the paper was performed to determine where along the beamline the beam quality was degrading and causing these losses in P2B. Finding where the beam quality is worsened early on in the beamline can help prevent beam loss that can quench superconducting components, cause outgassing, and damage parts that aren't designed to handle the energy deposited by the lost particles. If these instabilities can be fixed it will help the accelerator run more efficiently and reliably both at low and high beam currents.

II TRACK Beamline Simulations

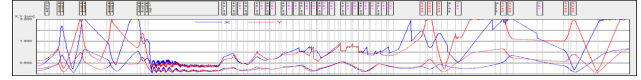
The TRACK Software TRACK is a prevalent beam dynamics simulation tool designed to study the propagation of ion beams through linear accelerators and beam transport lines. Version 3.9 was used for these tests. An accelerator beamline can be built in TRACK component by component and then, from a set of initial conditions, the beam can be propagated through the geometry and resulting dynamics can be observed. This is especially useful for operators who are basing their corrections on transmission values alone and have no means to visualize the beamline while the accelerator is running.

A Pepper-pot Data Analysis

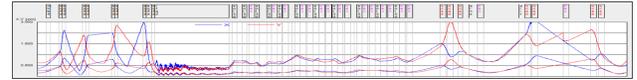
Pepper-pot Detector. The pepper-pot detector is composed of a thick metal plate with an even grid of small circular openings and a viewing screen a set distance from the metal plate. When the metal plate is moved to block the beam, only the particles that align with the openings in the plate will go on to drift and be measured on the screen. Since the distance between the holes in the screen is known, the distance between and orientation of the pattern of dots on the screen reveals information about the transverse properties of the beam.

ϵ_{xn} [π cm mrad]	0.041 ± 0.004
ϵ_{yn} [π cm mrad]	0.069 ± 0.008
α_x	0.23 ± 0.06
α_y	0.30 ± 0.05
β_x [cm/rad]	44 ± 6
β_y [cm/rad]	72 ± 9

Table 1: Beam initial conditions from pepper-pot detector.



(a) Simulation with Recorded Focusing Values



(b) Optimized Solenoid Values

Figure 3: TRACK output for the beam envelope through the entire relevant beamline.

Initial Beam Conditions. There is a Pepper-pot detector located at the start of the LEBT that was used to find the initial conditions of the beam for the TRACK simulations. Measurements with beam currents from 52nA to $5.2\mu\text{A}$ were conducted and a dedicated program was used to find the normalized emittance (ϵ_n), as well as the α and β Twiss parameters in the x and y phase spaces. This data is shown in Table 1.

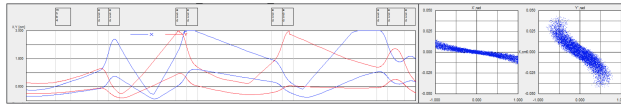
B Focusing Component Optimizations

Necessary Optimizations When the recorded focusing element values were input straight into TRACK, the beam became erratic, as seen in Figure 3.a, and by the end of P2B there was only 23.5% transmission compared to the measured transmission of 79.6%. The transmission loss per beamline section is shown in Table 2. In order to create simulations that could effectively model the March runs and provide a basis from which to compare the experimental transmission and emittance results, optimizations for transmission of the focusing elements in each beamline section were performed. The results of those optimizations are what follows.

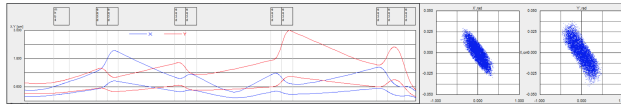
Recorded LEBT values in TRACK When the values recorded for the LEBT quadrupole magnets were input directly into TRACK, there was only 91.5% transmission. 100% transmission is expected for beam transport lines. Especially problematic was the final conditions of the LEBT going into the RFQ. These conditions did not match the acceptance of the RFQ and so only 31.5%

	Recorded Values (TRACK) % Transmission	Optimized Values (TRACK) % Transmission	Measured % Transmission
LEBT	91.5%	100.0%	100.0%
RFQ	31.5%	82.4%	(no measuring device)
PII	92.5%	100.0%	88.1%
P2B	88.0%	99.4%	90.3%
Total	23.5%	81.9%	79.6%

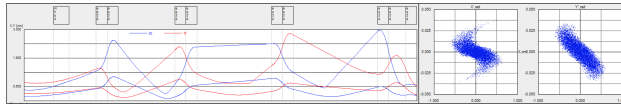
Table 2: Comparison of transmission values.



(a) Simulation with Recorded Quadrupole Values



(b) Low Voltage Optimized Quadrupole Values



(c) High Voltage Optimized Quadrupole Values

Figure 4: TRACK output for the beam envelope and emittance through LEBT. Emittance is skewed and 31.8% larger than the low voltage solution from the higher voltage quadrupole magnets in (c).

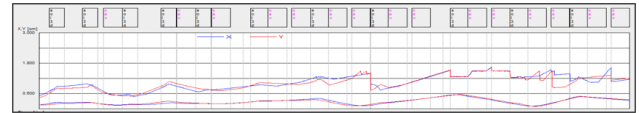
of the particles were effectively accelerated through the structure.

LEBT Optimization Results Using the Pepper-pot data as initial conditions and the acceptance of the RFQ as final conditions, TRACK was able to find a solution for the strengths of the quadrupole magnets that would optimize transmission. Two solutions were found, one using the recorded values as a starting point and another using lower initial conditions. Both solutions have 100% transmission, but the emittance of the higher voltage solution was 31.8% larger than the low voltage solution. The higher voltage emittance also had a less elliptical shape, the smearing can be seen in Figure 4.c, and would not transport as cleanly down the beamline. This larger and ill-shaped emittance could be major factor causing the transmission loss measured in P2B.

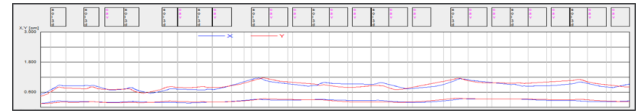
Recorded PII values in TRACK It can be seen from the erratic jumps in the width of the beam envelope in Figure 5.a that the beam is growing larger than the apertures of the elements and shearing is occurring, something preventable by tuning the solenoid values as shown in Figure 5.

	Recorded [kV]	LV Opt. [kV]	% Diff	HV Opt. [kV]	% Diff
QDP201	-10.36	-5.59	-46.0%	-9.40	-9.3%
	10.20	6.00	-41.2%	8.95	-12.3%
QDP202	-8.03	-5.23	-34.8%	-8.06	0.4%
	7.49	5.48	-26.9%	7.05	-5.9%
QDP203	5.27	7.61	44.4%	6.13	16.4%
	-5.97	-6.17	6.5%	-6.28	8.4%
QTP204	6.80	7.58	11.4%	8.99	32.2%
	-6.33	-7.54	19.0%	-7.33	15.8%
	2.81	7.06	151.2%	4.29	52.7%

Table 3: Recorded LEBT Quadrupole Strengths Compared to Optimized Values



(a) Simulation with Recorded Solenoid Values



(b) Optimized Solenoid Values

Figure 5: TRACK output for the beam envelope through PII.

PII Optimization Results Since during these tests the PII accelerating cavities were deactivated, PII can be considered another beam transport line and should have 100% transmission. To achieve this, the solenoids were manually tuned to maximize transmission and minimize the beam envelope. The change in intensity of the solenoids are listed in Table 4. These changes resulted in 100% transmission with only an average difference in solenoid strength of 20.1%. If an optimizing script were used a solution closer to the recorded values may have been found, but for the purposes of creating a simulation comparable to the measured data these changes were adequate.

Recorded P2B values in TRACK The resulting simulation from the recorded P2B values was quite erratic. Only 87.97% of the already low transmission beam made it through this section. The poor correlation earlier along the beamline was compounded going into P2B and the quadrupoles were not tuned to transport a beam of those initial conditions.

P2B Optimization Results The quadrupole focusing elements in the P2B beamline were manually adjusted using the TRACK software. The tuning of the quadrupoles increased the LV transmission from 88.0% to

	Recorded [Gs]	Optimized [Gs]	% Diff
sol3d 1	37128.00	39928.00	7.5%
sol3d 2	38188.80	31188.80	-18.3%
sol3d 3	37145.10	33145.10	-10.8%
sol3d 4	36650.64	30650.64	-16.4%
sol3d 5	21958.56	25958.56	18.3%
sol3d 6	20637.00	23637.00	14.5%
sol3d 7	30267.60	20267.60	-33.0%
sol3d 8	27516.00	24516.00	-10.9%
sol3d 9	25796.25	22796.25	-11.6%
sol3d 10	30382.25	16382.25	-46.1%
sol3d 11	30095.63	20095.63	-33.2%

Table 4: Recorded PII solenoid strengths compared to optimized values.

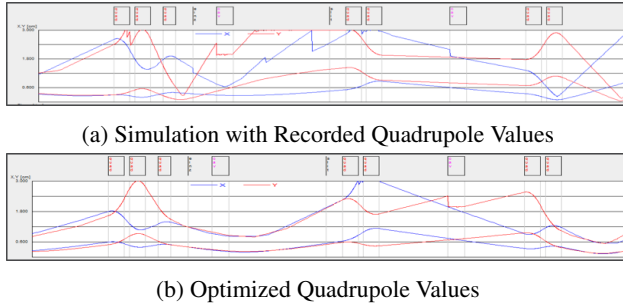


Figure 6: TRACK output for the beam envelope through P2B. The beam envelope through the optimized quadrupoles is much smoother, raising the transmission from 88.0% to 99.4%.

99.4%, much closer to the 100% transmission that should have been possible. The quadrupole magnets had relatively minor corrections averaging a 9.8% difference, as seen in Table 5. The beam envelopes also converge and become approximately symmetric, a property designed to occur at this point in the beamline and important to the quadrupole scan technique.

Conclusions After this final step in the ATLAS beamline optimization we have a simulation that is close enough to the measured transmission values to be used as a basis for emittance comparison with the analyzed quadrupole scan data.

III Quadrupole Scan Technique

A Beam and Transfer Matrix Formalism

Beam Ellipse. A beam of particles can be fully described in a six-dimensional phase space consisting of $\{x, y, z, p_x, p_y, p_z\}$, which when uncoupled can be broken

	Recorded [Gs]	Optimized [Gs]	% Diff
QDP 301	784.35	684.35	-12.7%
	-1300.00	-1000.00	-23.1%
QSP 301	871.88	624.35	-28.4%
QDP 302	-556.25	-556.25	0.0%
	565.63	590.63	4.4%
QDP 303	-730.00	-730.00	0.0%
	840.00	840.00	0.0%

Table 5: Recorded P2B quadrupole strengths compared to optimized values.

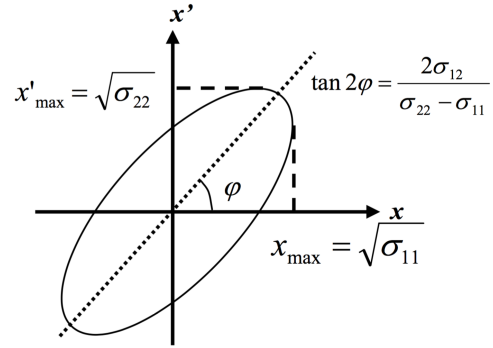


Figure 7: **Beam Ellipse.** Physical definitions of the geometric beam ellipse in phase space as described by equation 1. [2]

up into transverse and longitudinal phase spaces of the form $\{x, p_x\}$. The distribution of particles within each space can be considered bound by an ellipse described statistically by a beam matrix σ as shown in Figure 7.

$$\sigma = \begin{bmatrix} \sigma_{11} & \sigma_{12} \\ \sigma_{12} & \sigma_{22} \end{bmatrix} = \begin{bmatrix} \sigma_{x^2} & \sigma_{xx'} \\ \sigma_{xx'} & \sigma_{x'^2} \end{bmatrix} = \begin{bmatrix} \langle x^2 \rangle & \langle xx' \rangle \\ \langle xx' \rangle & \langle x'^2 \rangle \end{bmatrix} \quad (1)$$

Emittance. The emittance is a value that can be used to characterize and compare the quality of any beam of particles. The geometrical emittance can be described as the area of the ellipse, and equivalently the square root of the determinant of the beam matrix.

$$\epsilon_{rms} = \sqrt{\det(\sigma)} = \sqrt{\sigma_{11}\sigma_{22} - \sigma_{12}^2} \quad (2)$$

This emittance can be normalized by multiplying it by the relativistic β and γ . The format output by TRACK is four times this normalized rms emittance and so will be how the emittance is described throughout the analysis. The normalized emittance is a property of the beam that is conserved and in principle should not change as the beam is accelerated and focused. In practice space

charge forces, non-linear forces, and certain electromagnetic fields can cause emittance growth.

$$\varepsilon_{Nrms} = \beta \gamma \varepsilon_{rms} = \beta \gamma \sqrt{\det(\Sigma)} \quad (3)$$

Transfer Matrices. A set of matrices called transfer matrices can be used to describe the motion of particles in the beam as they pass through components of the beamline. These are defined below for a focusing quadrupole (M_{Qf}), a defocusing quadrupole (M_{Qd}), and a drift (M_{drift}).

$$M_{Qf} = \begin{bmatrix} \cos(\sqrt{\kappa}s) & \frac{1}{\sqrt{\kappa}}\sin(\sqrt{\kappa}s) \\ -\sqrt{\kappa}\sin(\sqrt{\kappa}s) & \cos(\sqrt{\kappa}s) \end{bmatrix}$$

$$M_{Qd} = \begin{bmatrix} \cosh(\sqrt{|\kappa|}s) & \frac{1}{\sqrt{|\kappa|}}\sinh(\sqrt{|\kappa|}s) \\ \sqrt{|\kappa|}\sinh(\sqrt{|\kappa|}s) & \cosh(\sqrt{|\kappa|}s) \end{bmatrix} \quad (4)$$

$$M_{drift} = \begin{bmatrix} 1 & s \\ 0 & 1 \end{bmatrix}$$

Where κ is the focusing strength of the quadrupole magnet defined as $\frac{B'}{B\rho}$ and s is longitudinal length of the element.

These matrices can be multiplied together to represent a sequence of elements along a beamline. The beam matrix can be propagated along a section of the beamline by multiplying it by the compound matrix describing the geometry of the beamline (M) and it's transpose.

$$\sigma(s) = M(s)\sigma(s_0)M(s)^T \quad (5)$$

Quadrupole Scan Formalism. The quadrupole scan is a technique used to calculate the transverse emittance of the beam. It uses the quadratic relationship between the focusing strength of a quadrupole magnet and the squared rms beam size to determine the emittance. Quadrupole scans are an extremely useful tool because they allow the emittance to be calculated at any point in the beamline there is a quadrupole magnet and a BPM. The data collected during the March 10th quadrupole scan was from a quadrupole doublet and BPM located at the end of the P2B line. The transfer matrices for this geometry can be described as

$$M = M_{drift}M_{Qd}M_{drift}M_{Qf} = \begin{bmatrix} M_{11} & M_{12} \\ M_{21} & M_{22} \end{bmatrix} \quad (6)$$

When the beam matrix is propagated along this geometry as described by equation 5, the first element σ_{11} of the beam matrix at the screen is described by

$$\sigma_{11}(s) = M_{11}^2\sigma_{11}(s_0) + 2M_{11}M_{12}\sigma_{12}(s_0) + M_{12}^2\sigma_{22}(s_0) \quad (7)$$

After multiple measurements of σ_{11} at the screen are taken at different quadrupole strengths, a system of equations with three unknowns ($\sigma_{11}(0)$, $\sigma_{12}(0)$, and $\sigma_{22}(0)$) develops. The system is fully constrained after three measurements, but more can be used to minimize error.

$$\begin{bmatrix} \sigma_{11(a)}(s) \\ \sigma_{11(b)}(s) \\ \dots \\ \sigma_{11(n)}(s) \end{bmatrix} = \begin{bmatrix} M_{11(a)}^2 & 2M_{11(a)}M_{12(a)} & M_{12(a)}^2 \\ M_{11(b)}^2 & 2M_{11(b)}M_{12(b)} & M_{12(b)}^2 \\ \dots & \dots & \dots \\ M_{11(n)}^2 & 2M_{11(n)}M_{12(n)} & M_{12(n)}^2 \end{bmatrix} \begin{bmatrix} \sigma_{11}(s_0) \\ \sigma_{12}(s_0) \\ \sigma_{22}(s_0) \end{bmatrix} \quad (8)$$

The matrix of transfer matrix components (A) is then simply inverted if there were three measurements, as shown in Equation 9,

$$A^{-1} \begin{bmatrix} \sigma_{11(a)}(s) \\ \sigma_{11(b)}(s) \\ \sigma_{11(c)}(s) \end{bmatrix} = \begin{bmatrix} \sigma_{11}(s_0) \\ \sigma_{12}(s_0) \\ \sigma_{22}(s_0) \end{bmatrix} \quad (9)$$

or a Moore-Penrose pseudo-inverse can be used to calculate a least squares fit for more than three measurements, as shown in Equation 10,

$$A^T(AA^T)^{-1} \begin{bmatrix} \sigma_{11(a)}(s) \\ \sigma_{11(b)}(s) \\ \dots \\ \sigma_{11(n)}(s) \end{bmatrix} = \begin{bmatrix} \sigma_{11}(s_0) \\ \sigma_{12}(s_0) \\ \sigma_{22}(s_0) \end{bmatrix} \quad (10)$$

and the emittance can be determined from the beam matrix at s_0 using Equation 2.[2] A MATLAB program was written to automate this calculation taking the quadrupole currents and x and y rms data as input.

B TRACK Quad Scan Simulation

Simulation Format In order to test the quad scan analysis program, a quadrupole scan of identical geometry to the end of the P2B line was built in TRACK. Both the x -focusing and y -focusing quadrupoles were scanned across a range of currents. The first scenario tested was centered about the smallest x_{rms} and y_{rms} values, an area called the beam waist. The next was centered about the y beam waist, but was far from the x waist, where the plotted values look more linear.

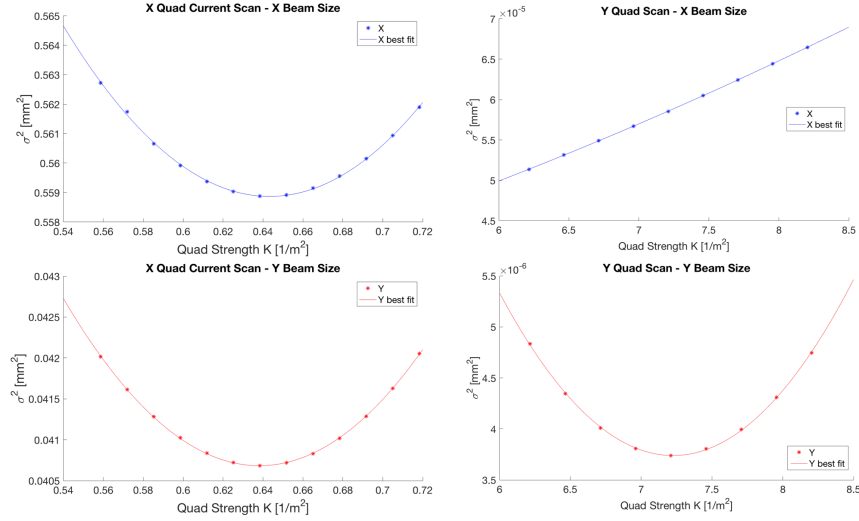


Figure 8: x and y rms beam size plotted against the focusing strength of the scanned quadrupole magnet. Comparison of simulated x -quad scan with a symmetric beam and a simulated y quad scan with an asymmetric beam.

	TRACK	Calculation	% Diff
ϵ_{xNrms} [mm mrad]	0.0693	0.0685	1.2%
ϵ_{yNrms} [mm mrad]	0.115	0.116	0.9%

Table 6: Comparison of simulated x -quadrupole scan emittance results between TRACK and analysis program where both x and y measurements are about the beam waist.

Symmetric Test Results The test run about the x and y beam waists was a scan in the x -focusing quadrupole with current values from 2.10A to 2.70A in increments of 0.15A. The results were extremely close to the TRACK simulation output. As shown in Table 6, both the x and y emittance were around a 1% difference from the TRACK output.

Asymmetric Test Results This scan was conducted by varying the y -focusing quadrupole current from 2.50A to 3.30A by 0.1A while maintaining the x -focusing quad at 2.35A. There was a vast difference in the result of this test from that of the symmetric scan. The results are shown in Table 7. The y values were scanned across the beam waist and once again there was agreement between TRACK and the program output. The x values were far from the beam waist and so resulted in a much less accurate approximation of the quadratic fit for the data, a 19.5% difference.

Conclusions from Quadrupole Scan Simulation. It is clear from these tests that the program is much more accurate when calculating the emittance from data that

	TRACK	Calculation	% Diff
ϵ_{xNrms} [mm mrad]	0.0693	0.0558	19.5%
ϵ_{yNrms} [mm mrad]	0.115	0.115	0.0%

Table 7: Comparison of simulated y -quadrupole scan emittance results between TRACK and analysis program where y scans across the beam waist, but x does not.

spans across the beam waist. Even with 9 data points, when the x_{rms} data spread did not span the waist the results varied by almost 20% from the TRACK output. When the points are far from the vertex of the parabola the points approximate a line and small changes in the alignment of these points due to measuring errors can compound and result in a huge change in the overall shape of the fitted parabola. This is valuable information for the March 10th quadrupole scan because neither the x -focusing nor y -focusing quadrupole scan were centered about both the x and y beam waists. Additionally, only 3 data points were taken for each scan, so statistical and measurement error plays a larger role than in these simulated tests.

C March 10th Quadrupole Scan Data Analysis

Beamline Parameters During Quad Scan The purpose of the run on March 10th was to measure the emittance at the end of the RFQ. There are no detectors that can directly measure the emittance, such as a pepperpot, located after the RFQ so indirect means were necessary. In order to maintain the emittance from the exit

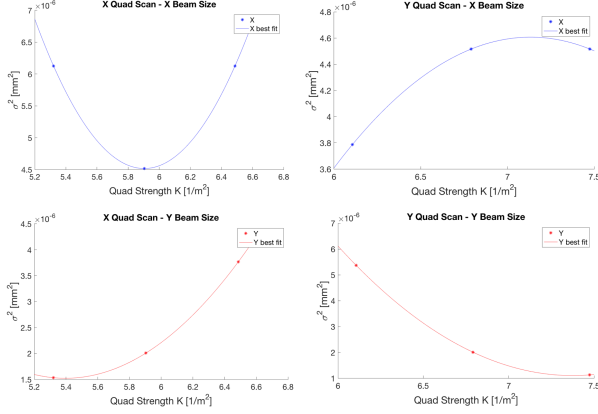


Figure 9: Comparison of x and y quad scan data from measurement. x and y rms data plotted against the focusing strength of the scanned quadrupole magnet.

	Pepper-pot	TRACK	X Quad Scan	Y Quad Scan	X-Y Avg.
ϵ_{xNrms} [mm mrad]	0.0700	0.158	0.0529	0.0706	0.0618
ϵ_{yNrms} [mm mrad]	0.1150	0.163	0.204	0.0945	0.1494

Table 8: Comparison of the initial emittance at the pepper-pot and the final emittance from TRACK and the quadrupole scan emittance values.

of the RFQ to the quadrupole doublet at the end of P2B where the scan was conducted, all of the accelerating and bunching cavities in PII were shut off. This way the accelerating fields would not introduce any instabilities and in principal the emittance would stay constant.

Emittance Comparison After testing the MATLAB program against the TRACK simulations and finding very good agreement, it was time to input the experimental data and compare it to both the emittance from the optimized TRACK simulation developed in Section II and the emittance calculated at the pepper-pot detector. The TRACK simulation saw slight emittance growth from the pepper-pot to the end of P2B, this growth is shown in Table 8. The quad scan results also listed in Table 8 demonstrate inconsistent agreement with the TRACK and pepper-pot data. The y -quad scan x emittance was very close to the pepper-pot value, within 1%, and the y emittance was only 17% different. The x -quad scan x emittance was smaller than both the pepper-pot and TRACK, while the y emittance was larger than both. In both the x and y planes from both quad scans the emittance was larger in y than in x , the same relationship as at the pepper-pot detector. The closest correspondence was between the quad scan and pepper-pot emittance values. This suggests that the emittance growth through the RFQ and from over-focusing in the LEBT in the TRACK sim-

ulation may not be experienced to the same degree in practice.

Sources of Error The inconsistency between TRACK, the pepper-pot and the quad scan calculation, shown in Table 8 must then have been caused by only conducting three measurements per quadrupole scan. A quadratic fit is fully constrained by three points, but with the level of uncertainty in these measurements, the accuracy of the quadratic relationship is low. The large disagreement between the x -quad and y -quad scan y emittance calculation (0.204mm-mrad compared to 0.0945mm-mrad) could have been caused by not sweeping the y profile across the beam waist. Figure 9 shows the y profile was swept to a minimum, not across the waist and so the extrapolation of the quadratic fit from that data is more susceptible to small variations in measurement.

IV Conclusion

Source of Transmission Loss Although it is impossible to know with complete certainty without implementing the change and observing the response from the beam, the beam loss measured in the P2B line could have been caused by the large emittance exiting the LEBT. This large emittance was caused by using higher quadrupole focusing strengths than needed. The lower emittance solution may not correspond directly to the values of the solution in the actual accelerator due to factors like misalignment, but finding this solution in track means that a similar solution is possible in practice.

Implementation of the Quadrupole Scan In order to obtain more accurate emittance measurements from future quadrupole scan data, a greater number of points need to be taken and care must be taken that the beam is swept across the beam waist in both transverse planes.

Future Projects Now that the emittance has been calculated to high accuracy from the simulated quadrupole scan and shown promising results when applied to real data, the method is trusted and may be implemented more in ATLAS in the future. The MATLAB program written to automate the calculation could be altered and integrated into the systems that already exist in ATLAS to allow for emittance measurements in areas where such a measurement hasn't been possible before. This will greatly aid the operators as they are working with the accelerator to provide the cleanest beam possible.

V Acknowledgements

Huge thanks to my mentors Brahim Mustapha and Clay Dickerson for their guidance throughout my research at Argonne National Laboratory.

References

- [1] N. et al. Development of a pepper-pot emittance meter for diagnostics of low-energy multiply charged heavy ion beams extracted from an ecr ion source., 2016.
- [2] S. Skelton. Multi-quadrupole scan for emittance determination at pitz.